U-9981

NATIONAL ADVISORY COMMITTEE FOR AERONAUTICS

REPORT No. 902

SUBSONIC FLOW OVER THIN OBLIQUE AIRFOILS AT ZERO LIFT

DTIC
SELECTED
SEP 0 6 1995
F

By ROBERT T. JONES

NAVY RESEARCH SECTION
SCIENCE DIVISION
REFERENCE DEPARTMENT
LIBRARY OF CONGRESS

1

6 JAN 1950

DISTRIBUTION STATEMENT A
Approved for public release
Distribution Unlimited

1948

For sale by the Superintendent of Documents, U. S. Government Printing Office, Washington 25, D. C. - - - - - Price 15 cents

19950831 108

DTIC QUALITY INSPECTED 5

AERONAUTIC SYMBOLS

1. FUNDAMENTAL AND DERIVED UNITS

	Symbol	Metric		English	
		Unit	Abbreviation	Unit	Abbreviation
Length	l	meter	m	foot (or mile)	ft (or mi)
Time	t	second	s	second (or hour)	sec (or hr)
Force	F	weight of 1 kilogram	kg	weight of 1 pound	lb
Power	P	horsepower (metric)		horsepower	hp
Speed	V	kilometers per hour	kph	miles per hour	mph
		meters per second	mps	feet per second	fps

2. GENERAL SYMBOLS

W Weight$=mg$

g Standard acceleration of gravity$=9.80665$ m/s^2 or 32.1740 ft/sec^2

m Mass$=\frac{W}{g}$

I Moment of inertia$=mk^2$. (Indicate axis of radius of gyration k by proper subscript.)

μ Coefficient of viscosity

ν Kinematic viscosity

ρ Density (mass per unit volume)

Standard density of dry air, 0.12497 kg-m^{-4}-s^2 at 15° C and 760 mm; or 0.002378 lb-ft^{-4} sec^2

Specific weight of "standard" air, 1.2255 kg/m^3 or 0.07651 lb/cu ft

3. AERODYNAMIC SYMBOLS

S Area

S_w Area of wing

G Gap

b Span

c Chord

A Aspect ratio, $\frac{b^2}{S}$

V True air speed

q Dynamic pressure, $\frac{1}{2}\rho V^2$

L Lift, absolute coefficient $C_L=\frac{L}{qS}$

D Drag, absolute coefficient $C_D=\frac{D}{qS}$

D_0 Profile drag, absolute coefficient $C_{D_0}=\frac{D_0}{qS}$

D_i Induced drag, absolute coefficient $C_{D_i}=\frac{D_i}{qS}$

D_p Parasite drag, absolute coefficient $C_{D_P}=\frac{D_p}{qS}$

C Cross-wind force, absolute coefficient $C_C=\frac{C}{qS}$

i_w Angle of setting of wings (relative to thrust line)

i_t Angle of stabilizer setting (relative to thrust line)

Q Resultant moment

Ω Resultant angular velocity

R Reynolds number, $\rho\frac{Vl}{\mu}$ where l is a linear dimension (e.g., for an airfoil of 1.0 ft chord, 100 mph, standard pressure at 15° C, the corresponding Reynolds number is 935,400; or for an airfoil of 1.0 m chord, 100 mps, the corresponding Reynolds number is 6,865,000)

α Angle-of attack

ϵ Angle of downwash

α_o Angle of attack, infinite aspect ratio

α_i Angle of attack, induced

α_a Angle of attack, absolute (measured from zero-lift position)

γ Flight-path angle

REPORT No. 902

SUBSONIC FLOW OVER THIN OBLIQUE AIRFOILS AT ZERO LIFT

By ROBERT T. JONES

Ames Aeronautical Laboratory
Moffett Field, California

Accesion For
NTIS CRA&I ☑
DTIC TAB ☐
Unannounced ☐
Justification .....
By .....
Distribution /
Availability Codes
Dist | Avail and / or Special
A-1

National Advisory Committee for Aeronautics

Headquarters, 1724 F Street NW, Washington 25, D. C.

Created by act of Congress approved March 3, 1915, for the supervision and direction of the scientific study of the problems of flight (U. S. Code, title 50, sec. 151). Its membership was increased to 17 by act approved May 25, 1948. (Public Law 549, 80th Congress). The members are appointed by the President, and serve as such without compensation.

JEROME C. HUNSAKER, Sc. D., Cambridge, Mass., *Chairman*

ALEXANDER WETMORE, Sc. D., Secretary, Smithsonian Institution, *Vice Chairman*

HON. JOHN R. ALISON, Assistant Secretary of Commerce.

DETLEV W. BRONK, PH. D., President, Johns Hopkins University.

KARL T. COMPTON, PH. D. Chairman, Research and Development Board, National Military Establishment.

EDWARD U. CONDON, PH. D., Director, National Bureau of Standards.

JAMES H. DOOLITTLE, Sc. D., Vice President, Shell Union Oil Corp.

R. M. HAZEN, B. S., Director of Engineering, Allison Division, General Motors Corp.

WILLIAM LITTLEWOOD, M. E., Vice President, Engineering, American Airlines, Inc.

THEODORE C. LONNQUEST, Rear Admiral, United States Navy, Assistant Chief for Research and Development, Bureau of Aeronautics.

EDWARD M. POWERS, Major General, United States Air Force, Assistant Chief of Air Staff–4.

JOHN D. PRICE, Vice Admiral, United States Navy, Deputy Chief of Naval Operations (Air).

ARTHUR E. RAYMOND, M. S., Vice President, Engineering, Douglas Aircraft Co., Inc.

FRANCIS W. REICHELDERFER, Sc. D., Chief, United States Weather Bureau.

HON. DELOS W. RENTZEL, Administrator of Civil Aeronautics, Department of Commerce.

HOYT S. VANDENBERG, General, Chief of Staff, United States Air Force.

THEODORE P. WRIGHT, Sc. D., Vice President for Research, Cornell University.

HUGH L. DRYDEN, PH. D., *Director of Aeronautical Research*

JOHN W. CROWLEY, JR., B. S., *Associate Director of Aeronautical Research*

JOHN F. VICTORY, LL.M., *Executive Secretary*

E. H. CHAMBERLIN, *Executive Officer*

HENRY J. E. REID, Eng. D., Director, Langley Aeronautical Laboratory, Langley Field, Va.

SMITH J. DEFRANCE, B. S., Director, Ames Aeronautical Laboratory, Moffett Field, Calif.

EDWARD R. SHARP, Sc. D., Director, Lewis Flight Propulsion Laboratory, Cleveland Airport, Cleveland, Ohio

---

TECHNICAL COMMITTEES

AERODYNAMICS
POWER PLANTS FOR AIRCRAFT
AIRCRAFT CONSTRUCTION
OPERATING PROBLEMS
INDUSTRY CONSULTING

Coordination of Research Needs of Military and Civil Aviation
Preparation of Research Programs
Allocation of Problems
Prevention of Duplication
Consideration of Inventions

LANGLEY AERONAUTICAL LABORATORY, Langley Field, Va.

LEWIS FLIGHT PROPULSION LABORATORY, Cleveland Airport, Cleveland, Ohio

AMES AERONAUTICAL LABORATORY, Moffett Field, Calif.

Conduct, under unified control, for all agencies, of scientific research on the fundamental problems of flight

---

OFFICE OF AERONAUTICAL INTELLIGENCE, Washington, D. C.

Collection, classification, compilation, and dissemination of scientific and technical information on aeronautics

REPORT No. 902

SUBSONIC FLOW OVER THIN OBLIQUE AIRFOILS AT ZERO LIFT

By Robert T. Jones

SUMMARY

A previous report gave calculations for the pressure distribution over thin oblique airfoils at supersonic speed. The present report extends the calculations to subsonic speeds.

It is found that the flows again can be obtained by the superposition of elementary conical flow fields. In the case of the swept-back wing the pressure distributions remain qualitatively similar at subsonic and supersonic speeds. Thus a distribution similar to the Ackeret type of distribution appears on the root sections of the swept-back wing at $M=0$. The resulting positive pressure drag on the root section is balanced by negative drags on outboard sections.

INTRODUCTION

So far as is known, attempts to extend airfoil pressure-distribution calculations to three-dimensional flow have been confined to cases of thin lifting surfaces. It has generally been assumed that the component of the pressure distribution arising from the thickness of the airfoil will be but little affected by the finite span, or aspect ratio, of the wing. This supposition is borne out by the known incompressible-flow solutions for flat ellipsoids. These solutions show that the usual variations of aspect ratio produce small effects.

Compressible-flow theory shows, however, that the effects of plan form become more pronounced at higher speeds. The theory indicates a progressive reduction of the equivalent aspect ratio as the Mach number approaches 1.0. Hence at these speeds the three-dimensional character of the flow can no longer be neglected. Of particular interest are the deviations from two-dimensional flow near the root sections of a swept-back wing, since the adverse effects of compressibility may arise first in this region.

In the present report three-dimensional flows are obtained from a distribution of "pressure sources" in the chord plane of the airfoil. The shapes thus obtained are symmetrical airfoils at zero lift. The calculations are simplified by considering airfoils composed of conical or cylindrical surfaces. In these cases the sources can be arranged into lines of uniform strength following the generators of the surface. The relation between the strengths of the line sources and the shape of the airfoil is the same as in reference 1; that is, each line source produces a deflection of the streamlines crossing over the source. The pressure field of the line source again can be represented by systems of straight rays of equal pressure (isobars) radiating from the ends of the line source.

In general, the present development follows closely that of reference 1 and the reader should consult that report for additional details of the method. The solutions are given explicitly for $M=0$ but are extended to other Mach numbers by the well-known Prandtl transformation.

THE OBLIQUE LINE SOURCE

It is well known that an individual velocity component of a potential flow will satisfy the same differential equation as the potential. In the approximation of the thin-airfoil theory the pressure depends only on the individual component u, that is,

$$\frac{\Delta p}{q}=\frac{2u}{V} \tag{1}$$

while the slope of the surface depends only on the individual component w, that is

$$\frac{dz}{dx}=\frac{w}{V} \tag{2}$$

(See appendix for symbols.) Hence in the thin-airfoil theory it is often more convenient to deal directly with the velocities u and w as solutions of Laplace's equation than to derive these components from a velocity potential φ.

Since u is proportional to the pressure, a solution of Laplace's equation can represent directly the pressure distribution, hence the term "pressure potential." In this terminology, the fundamental solution

$$u=\frac{1}{r}=\frac{1}{\sqrt{x^2+y^2+z^2}} \tag{3}$$

represents a point source of pressure rather than a point source of fluid.

To get the effect of a row of sources, or a line source, along the x axis between the points a and b, it is necessary to integrate equation (3):

$$u=\int_a^b \frac{d\xi}{\sqrt{(x-\xi)^2+y^2+z^2}}$$

$$=\sinh^{-1}\frac{x-b}{\sqrt{y^2+z^2}}-\sinh^{-1}\frac{x-a}{\sqrt{y^2+z^2}} \tag{4}$$

The pressure field of the finite line source thus consists of the sum of two conical pressure fields radiating from the ends of the line source. (See fig. 1.) In the supersonic case (reference 1), the radial isobars forming the conical field were

843314—49

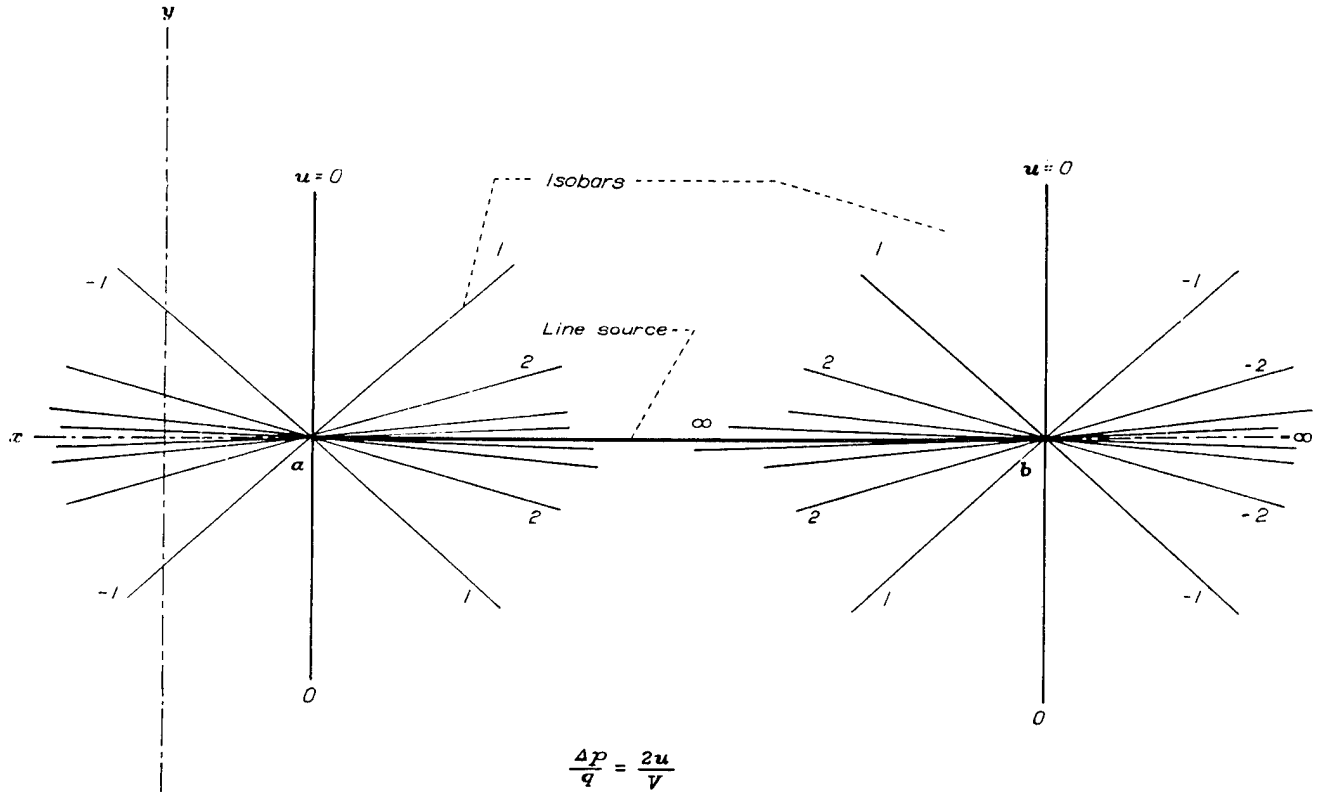

FIGURE 1.—Pressure field for line source of length $(b-a)$.

confined to the downstream Mach cone. Here, however, the isobars extend over the whole space.[1]

If the direction of flight is along the axis of the source (x axis), the flow will satisfy the boundary condition for a body of revolution. However, if the line source is turned out to a position oblique to the stream, the boundary shape will be distorted and, if the angle of obliquity is large enough to place the line source well outside the diameter of the original body, the figure formed will be an oblique wedge. The nose angle of the wedge is formed where the streamlines of the main flow cross the line source.

At supersonic speeds the expression for the oblique line source was obtained by applying an equivalent of the Lorentz transformation, for which the wave equation is invariant. The equivalent transformation for Laplace's equation is a rotation of the axes, given by

$$x' = x + my$$
$$y' = y - mx$$
$$z' = z\sqrt{1+m^2}$$

where m is the slope of the new axes relative to the old. (Note that a change of scale is admitted for convenience.) The geometry of the pressure field relative to the line source is not altered in any way by this rotation and the isobars behave as though they were rigidly attached to the ends of the source. For a line source with one end at the origin, we have

$$u = \sinh^{-1}\frac{x'}{\sqrt{(y')^2+(z')^2}} \tag{5}$$

This field is illustrated in figure 2 for the plane $z=0$. As $m \to \infty$ the x and y axes interchange and there is obtained

$$u = \sinh^{-1}\frac{y}{\sqrt{x^2+z^2}} \tag{6}$$

for a line source along y.

The vertical velocity w near $z=0$, which determines the shape of the boundary, may be found by integrating u with respect to x and then differentiating the resulting velocity potential with respect to z.

$$w = -\frac{\partial \phi}{\partial z} = \frac{\partial}{\partial z}\int_{-\infty}^{x} u\,dx \tag{7}$$

Evaluation of this integral for the overlapping fields from two ends of a line source gives

$$w = \pm 2\pi\frac{\sqrt{1+m^2}}{m} \tag{8}$$

over the area of the xy plane behind the line source.

[1] The conical pressure field for either the subsonic or the supersonic line source may be obtained directly from the general solutions of Laplace's equations of zero degree in x, y, z given by W. F. Donkin. (See reference 2, page 357.) The general solution is

$$u = f\left(\frac{y \pm iz}{x+\sqrt{x^2+y^2+z^2}}\right)$$

The solution corresponding to the subsonic line source is

$$u = -B.P.\log\frac{y+iz}{x+\sqrt{x^2+y^2+z^2}} = \sinh^{-1}\frac{x}{\sqrt{y^2+z^2}}$$

while the field for the supersonic source is given by

$$u = -B.P.\log\frac{y+iz}{x+\sqrt{x^2-y^2-z^2}} = \cosh^{-1}\frac{x}{\sqrt{y^2+z^2}}$$

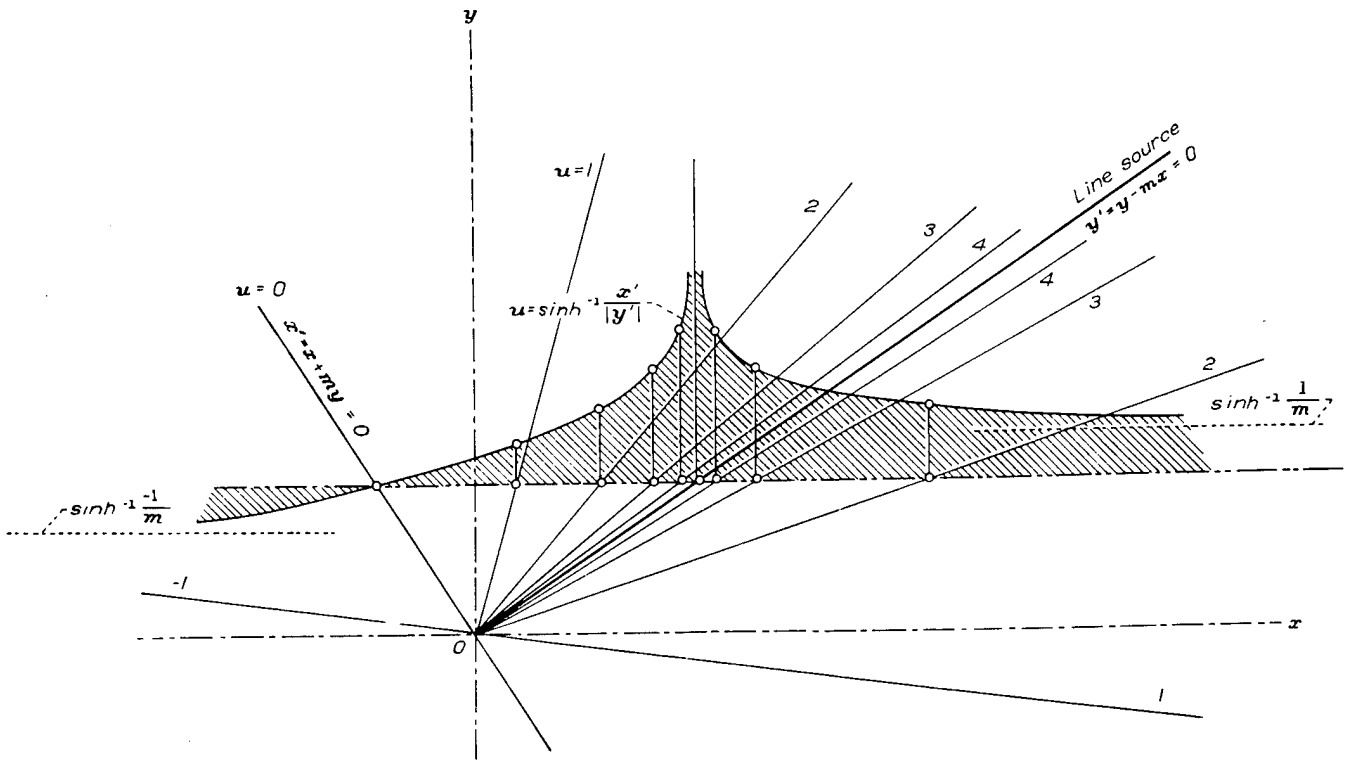

FIGURE 2.—Pressure field due to one end of oblique line source.

The figure formed by the streamlines crossing a line source is thus a wedge-shaped body having an oblique leading edge and extending indefinitely downstream. It is evident from equation (3) that the infinitely wide wedge cannot be treated in subsonic flow, since it creates an infinite pressure disturbance at all points.

The slope of the wedge surface away from the chord plane is given by

$$\frac{dz}{dx}=\frac{w}{V} \tag{9}$$

With this relation and equation (8) the pressure coefficient near the plane $z=0$ may be expressed in terms of the slope

$$\frac{\Delta p}{q}=\frac{1}{\pi}\frac{m}{\sqrt{1+m^2}}\frac{dz}{dx}\left(\sinh^{-1}\frac{x'-b'}{|y'|}-\sinh^{-1}\frac{x'-a'}{|y'|}\right) \tag{10}$$

where $|y'|$ indicates the absolute magnitude of y'. Following the thin-airfoil theory, the pressure over the chord plane ($z\to 0$) is taken as the pressure over the actual airfoil surface.

AIRFOILS BOUNDED BY PLANE SURFACES

It was seen that the effect of a line source in the pressure field is to cause a deflection of the streamlines crossing the source. The deflection thus produced is equal and opposite at points above and below the chord plane, so that the source spreads the streamlines apart. If the source is followed by a sink of equal strength, an equal opposite deflection of the streamlines will occur as they cross over the sink. The figure formed by the streamlines near the plane $z=0$ will thus be a plate of uniform thickness with a beveled leading edge.[2] (See fig. 3.)

[2] According to the thin-airfoil theory the thickness of the figure ends abruptly at the ends of the source lines. A more exact consideration would be expected to show some rounding at the tips of the wedge as indicated in figure 3.

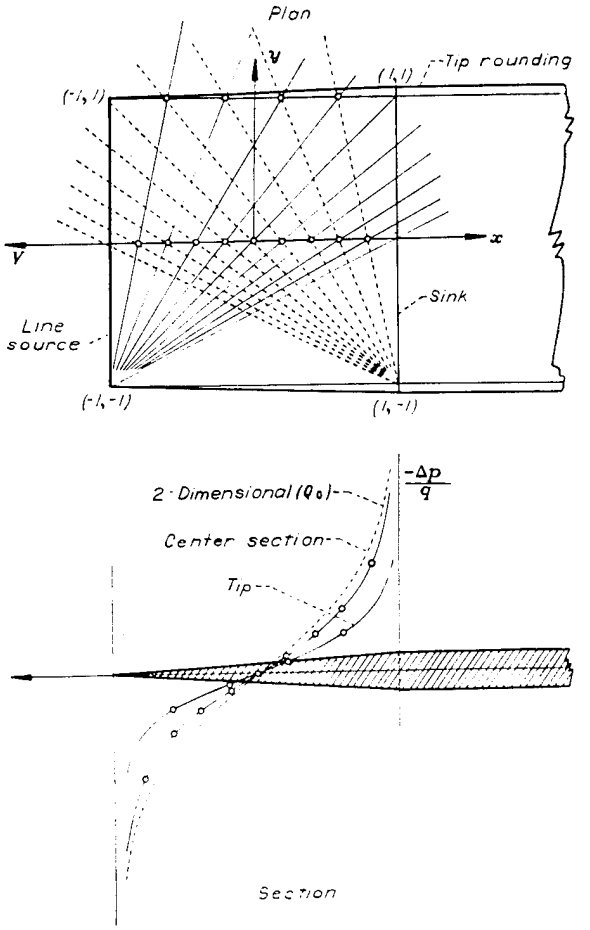

FIGURE 3.—Construction of the pressure distribution over a beveled leading edge.

The pressure distribution over such a beveled edge may be obtained very simply by superimposing the pressures laid off on radial isobars originating from the four corners of the bevel. Figure 3 illustrates this process for a bevel having a square plan form. Only isobars from one tip are shown because of the symmetry of the figure.

In figure 3, the line source and the line sink are parallel to the y axis, hence

$$u=\sinh^{-1}\frac{y+1}{|x+1|}-\sinh^{-1}\frac{y-1}{|x+1|}-\sinh^{-1}\frac{y+1}{|x-1|}+\sinh^{-1}\frac{y-1}{|x-1|} \tag{11}$$

It can be seen that if the aspect ratio of the figure is increased to a large value the ends of the line sources will be separated by a great distance and the isobars in intermediate regions will approach parallel straight lines, hence the flow field approaches a cylindrical or two-dimensional form. At the same time the arguments $y\pm1/|x\pm1|$ in equation (11) become $y\pm\eta/x\pm1$ and η takes on very large values so that

$$\sinh^{-1}\frac{y\pm\eta}{|x\pm1|}\rightarrow\pm\log 2\frac{y\pm\eta}{|x\pm1|}$$

and equation (11) is found to approach the Legendre function Q_0, that is

$$u=2\log\frac{|x-1|}{|x+1|}=-4\,Q_0(x) \tag{12}$$

(See reference 3, p. 110.)

This expression when combined with equation (8) agrees with the two-dimensional potential function for the wedge, that is,

$$-(u-iw)=4\,Q_0(x)\pm2\pi i\,P_0(x) \tag{13}$$

(See fig. 4.)

The isobars at right angles to the axis of the line source are lines of zero pressure, hence the rays originating at the tip of a rectangular wing contribute nothing to the pressure distribution at this tip. The whole pressure distribution at one tip is thus obtained by considering only those isobars radiating from the opposite tip. It is evident that in the case of a long narrow rectangular wing the pressures at either tip will be approximately one-half the pressures over the middle portion of the wing.

In case the wing is oblique the tip sections will no longer be at right angles to the axes of the source lines and the rays originating from the adjacent ends of the source lines *will* contribute to the pressure over the tip. It can be shown that this component of the tip pressure distribution is similar in form to the Ackeret type of distribution, that is, the pressure at any point of the surface is proportional to the slope of the surface at that point.

Consider first the sloping surface formed by a pair of oblique source-sink lines. The tip section lies along the lines of constant pressure of magnitude proportional to $\sinh^{-1}1/m$. Between the source and sink the pressures are additive, so that

$$\frac{\Delta p}{q}=\frac{2}{\pi}\frac{m}{\sqrt{1+m^2}}\frac{dz}{dx}\sinh^{-1}\frac{1}{m} \tag{14}$$

Ahead of or behind this section the pressures cancel.

In case of a curved airfoil surface the chord can be divided into elements composed of source-sink pairs, the strengths of which are proportional to the slope of the surface at the point in question. Each pair then contributes a pressure proportional to the local slope and contributes no pressure at other points. Hence, equation (14) applies when dz/dx is variable along the chord.

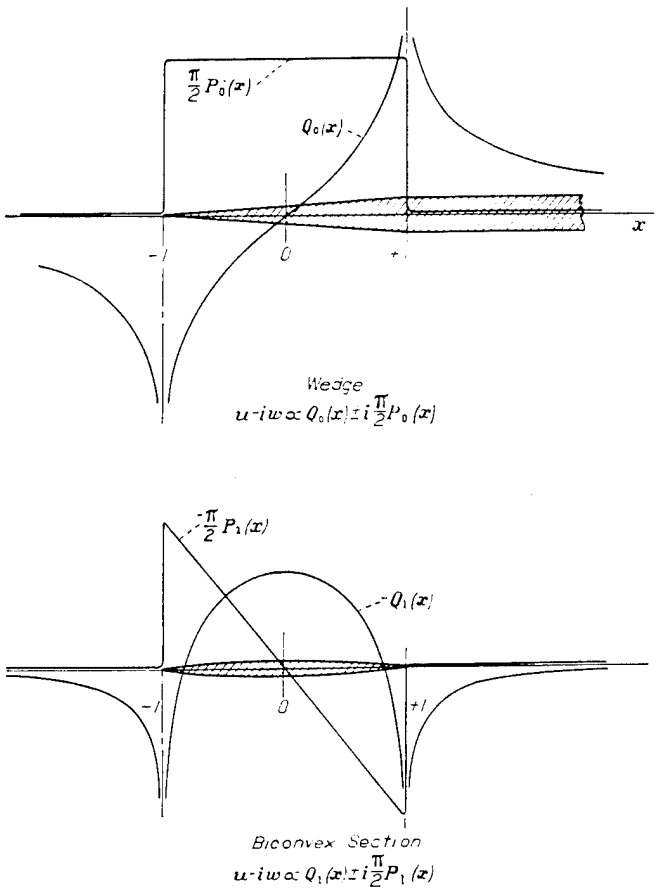

FIGURE 4.—Two-dimensional velocity functions for wedge and biconvex sections.

The foregoing arguments of course apply only at the tip section of the oblique wing. At some distance from the tip section the overlapping isobars radiating from the tip again produce a quasi-cylindrical pressure field as in the case of the rectangular wing. Thus the resultant pressure distribution at either tip of a long oblique wing consists of two components, one given by equation (14) and of the Ackeret type while the other component is equal to one-half the normal two-dimensional pressure distribution associated with the airfoil section.

Figure 5 shows the pressures over a beveled-edge profile having 45° sweepback. The pressure distribution over the root section is given by

$$\frac{\Delta p}{q}=\frac{-4}{\pi}\frac{m}{\sqrt{1+m^2}}\frac{dz}{dx}\left[Q_0(x)-\sinh^{-1}\frac{1}{m}P_0(x)\right] \tag{15}$$

at a great distance from either root or tip by

$$\frac{\Delta p}{q}=\frac{-4}{\pi}\frac{m}{\sqrt{1+m^2}}\frac{dz}{dx}Q_0(x) \tag{16}$$

and at the tip by

$$\frac{\Delta p}{q}=\frac{-2}{\pi}\frac{m}{\sqrt{1+m^2}}\frac{dz}{dx}\left[Q_0(x)+\sinh^{-1}\frac{1}{m}P_0(x)\right] \tag{17}$$

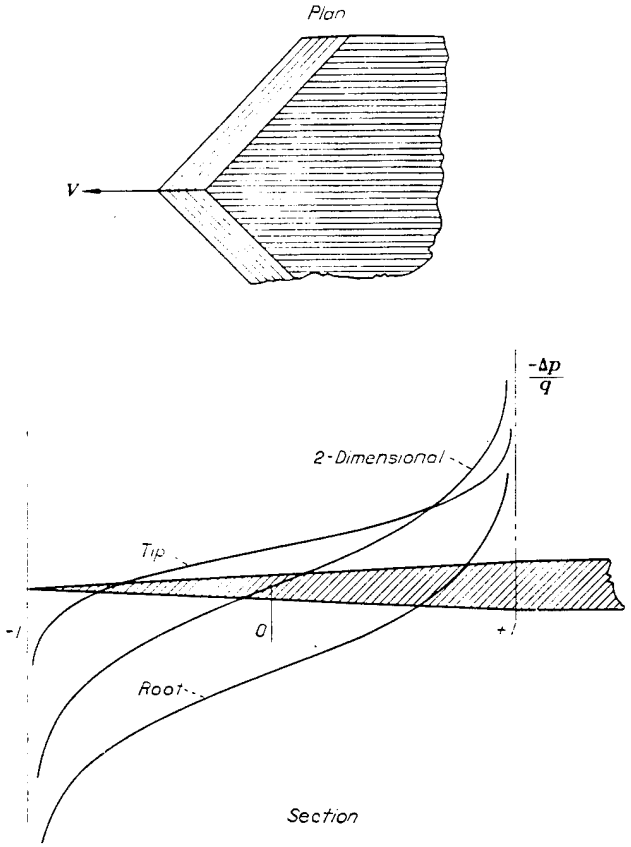

FIGURE 5.—Pressure distribution over beveled edge with 45° sweepback.

To take account of the effect of compressibility we make use of the Prandtl transformation, increasing both the x dimensions and the pressure coefficients by the factor $\frac{1}{\sqrt{1-M^2}}$. Replacing m by $\sqrt{1-M^2}\cot\Lambda$, where Λ is the angle of sweepback, equation (16) reduces to

$$\frac{\Delta p}{\rho/2(V\cos\Lambda)^2}=\frac{-4}{\pi}\frac{1}{\sqrt{1-(M\cos\Lambda)^2}}\frac{dz}{d(x\cos\Lambda)}Q_0(x) \tag{18}$$

Thus, at a great distance from either root or tip, the pressures follow a variation indicated by the normal component of velocity $V\cos\Lambda$.

At the root section, a component representing the Ackeret type of pressure distribution is added to equation (18). This component is

$$\frac{4}{\pi}\frac{1}{\sqrt{1-(M\cos\Lambda)^2}}\frac{dz}{d(x\cos\Lambda)}\sinh^{-1}\left(\frac{1}{\sqrt{1-M^2}\cot\Lambda}\right)P_0(x) \tag{19}$$

The factor $\sinh^{-1}\frac{1}{\sqrt{1-M^2}\cot\Lambda}$ shows a logarithmic infinity at $M=1.0$. Hence the pressure on the root section increases more rapidly with Mach number than do the pressures at other sections of the swept-back wing. Furthermore, the shape of the pressure distribution over the root section approaches the Ackeret shape more closely as the Mach number approaches 1.0. As shown in reference 1, the pressure distribution on the root section is exactly this shape at supersonic speeds, that is,

$$\frac{\Delta p}{q\cos^2\Lambda}=\frac{4}{\pi}\frac{1}{\sqrt{1-(M\cos\Lambda)^2}}\frac{dz}{d(x\cos\Lambda)}\cosh^{-1}\left(\frac{1}{\sqrt{M^2-1}\cot\Lambda}\right)P_0(x) \tag{20}$$

Since $\sinh^{-1}\to\cosh^{-1}$ for large values of the argument, the swept-back airfoil shows no discontinuity in the type of pressure distribution on passing through the speed of sound. It will be evident that similar reasoning can be applied to the tip sections.

AIRFOIL OF BICONVEX SECTION

The use of a finite number of sources and sinks results in airfoil sections composed of straight segments. Such sections are undesirable, since they show infinite pressure peaks at the bends in the surface. Surfaces having continuous curvature require continuous distribution of sources and sinks alined with the generators of the surface. The simplest of these is the biconvex profile in which the upper and lower surfaces are parabolic arcs and have constant curvature. Such a profile requires line sources of finite strength to form the desired angles of intersection of the arcs at the leading and trailing edges together with a uniform distribution of sinks along the chord plane between the two sources.

The pressure field for a uniform sheet of line sources is obtained by integrating the field of a single line source in the x direction. This integral is

$$\frac{1}{D}u=\int\sinh^{-1}\frac{x'}{|y'|}dx=\frac{\sqrt{1+m^2}}{m}y\sinh^{-1}\frac{x}{|y|}-\frac{1}{m}y'\sinh^{-1}\frac{x'}{|y'|} \tag{21}$$

The integration for a source sheet is actually somewhat simpler if the interference of a bilaterally symmetrical arrangement of sources is considered simultaneously. The influence of the symmetrical, or conjugate, arrangement is obtained by substituting $-m$ for m in equation (21). Denoting $x-my$ by $\bar{x}'$ and $y+mx$ by $\bar{y}'$ we have

$$\frac{1}{D}(u+\bar{u})=\int\left(\sinh^{-1}\frac{x'}{|y'|}+\sinh^{-1}\frac{\bar{x}'}{|\bar{y}'|}\right)dx=\frac{1}{m}\left(\bar{y}'\sinh^{-1}\frac{\bar{x}'}{|\bar{y}'|}-y'\sinh^{-1}\frac{x'}{|y'|}\right) \tag{22}$$

To obtain a complete swept-back wing it is necessary to add a number of component pressure fields as explained in

reference 1. For an infinite swept-back wing with leading and trailing edges at $y'=+m$ and $-m$, respectively, on one side, and at $\overline{y}'=+m$ and $-m$, respectively, on the other side, there is obtained

$$\frac{\Delta p}{q}=\frac{2}{\pi}\frac{m}{\sqrt{1+m^2}}\left(\frac{t}{c}\right)_{max}\left[\frac{y'}{m}\left(\sinh^{-1}\frac{x'+1}{|y'-m|}-\sinh^{-1}\frac{x'-1}{|y'+m|}\right)+\frac{\overline{y}'}{m}\left(\sinh^{-1}\frac{\overline{x}'-1}{|\overline{y}'-m|}-\sinh^{-1}\frac{\overline{x}'+1}{|\overline{y}'+m|}\right)+2Q_1\left(\frac{y'}{m}\right)+2Q_1\left(\frac{\overline{y}'}{m}\right)\right] \quad (23)$$

where $\left(\frac{t}{c}\right)_{max}$ is the thickness-chord ratio of the biconvex profile. The terms $Q_1\left(\frac{y'}{m}\right)$ represent the pressure distribution on the biconvex airfoil in two-dimensional flow. The appearance of these terms is the result of the assumption that the tips are removed to a great distance.

At the root section ($y=0$) equation (23) reduces to

$$\frac{\Delta p}{q}=\frac{2}{\pi}\frac{m}{\sqrt{1+m^2}}\left(\frac{t}{c}\right)_{max}\left[4Q_1(x)-4\sinh^{-1}\frac{1}{m}P_1(x)\right] \quad (24)$$

Figure 6 shows pressure distributions at various stations along the span for a biconvex wing with 60° sweepback. The curves assume the two-dimensional form at a relatively short distance ($y\cong\frac{1}{2}c$) from the root section, and similar behavior is to be expected near the tips. Hence the assumption of infinite aspect ratio should apply very nearly at any section situated more than one-half chord length from either root or tip.

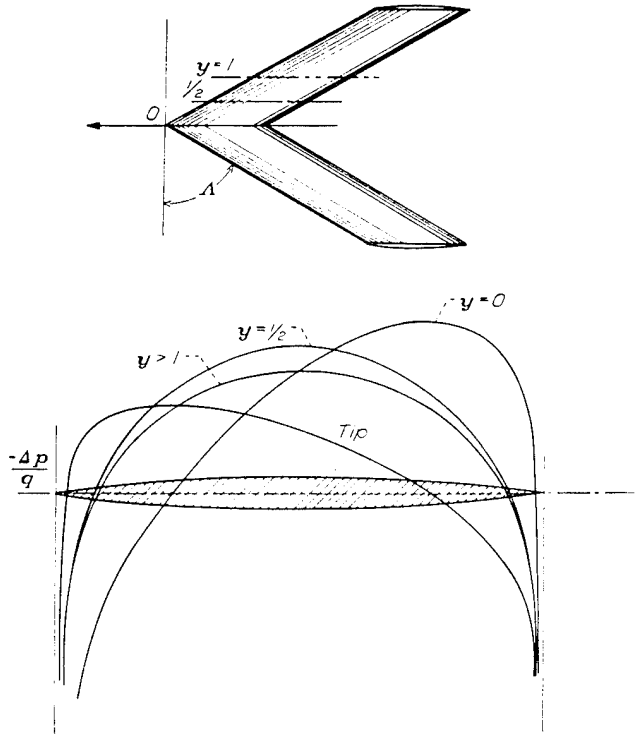

FIGURE 6.—Pressure distribution at various spanwise stations on swept-back wing, $\Lambda=60°$, $M=0$.

Figure 7 shows the effect of Mach number on the pressures over the root section and illustrates the progressive change to the supersonic type as the Mach number approaches 1.0. It can be seen that an increase in Mach number will not only increase the distortion of the pressure distribution but will increase the extent of the distortion along the span.

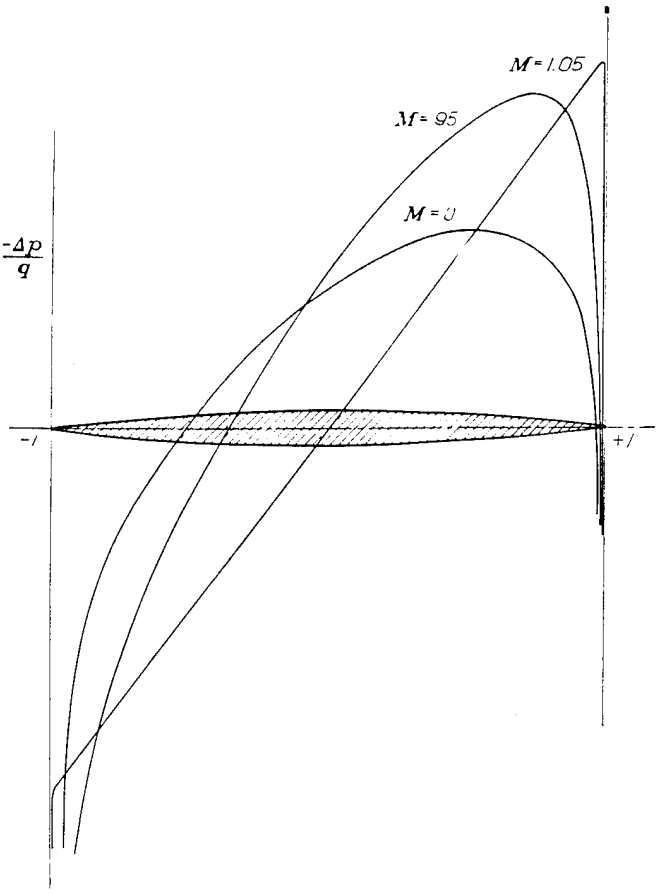

FIGURE 7.—Effect of Mach number on pressure distribution over root section of swept-back wing, $\Lambda=60°$, biconvex section.

An interesting point to be noted is that not all sections of the swept-back wing have zero pressure drag. A positive drag appears on the root sections and a negative drag on the tip sections. Hence the spanwise drag distribution is qualitatively similar to that at supersonic speeds though, of course, the net subsonic pressure drag is zero.

AMES AERONAUTICAL LABORATORY,
NATIONAL ADVISORY COMMITTEE FOR AERONAUTICS,
MOFFETT FIELD, CALIF., *May 1947*.

APPENDIX

SYMBOLS

V	flight velocity
M	Mach number
x, y, z	coordinates
ξ	point on x axis
η	point on y axis
ϕ	disturbance-velocity potential
u, v, w	disturbance-velocity components
p	local pressure
q	dynamic pressure $\left(\frac{1}{2}\rho V^2\right)$
ρ	air density
P_n, Q_n	Legendre functions
D	differential operator (d/dx)
t	thickness of wing
c	chord of wing (measured along x)
m	slope of line source (absolute value)
x'	$x+my$
y'	$y-mx$
$\bar{x}'$	$x-my$
$\bar{y}'$	$y+mx$
$R.\ P.$	Real part

REFERENCES

1. Jones, Robert T.: Thin Oblique Airfoils at Supersonic Speed. NACA Rep. No. 851, 1946.
2. Bateman, H.: Partial Differential Equations of Mathematical Physics. Dover Pub., 1944, p. 357.
3. Jahnke, Eugene, and Emde, Fritz: Tables of Functions with Formulas and Curves. Rev. Ed., Dover Pub., New York, 1943, pp. 107–117.

U. S. GOVERNMENT PRINTING OFFICE, 1949

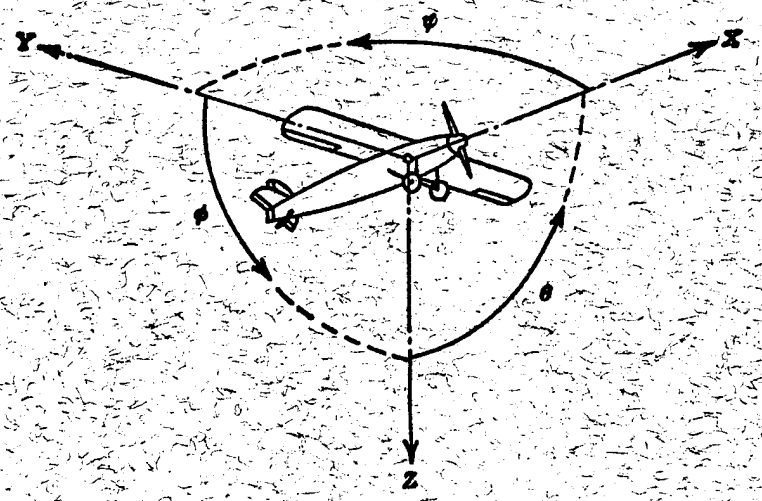

Positive directions of axes and angles (forces and moments) are shown by arrows

Axis		Force (parallel to axis) symbol	Moment about axis			Angle		Velocities	
Designation	Symbol		Designation	Symbol	Positive direction	Designation	Symbol	Linear (component along axis)	Angular
Longitudinal	X	X	Rolling	L	Y ⟶ Z	Roll	ϕ	u	p
Lateral	Y	Y	Pitching	M	Z ⟶ X	Pitch	θ	v	q
Normal	Z	Z	Yawing	N	X ⟶ Y	Yaw	ψ	w	r

Absolute coefficients of moment

$C_l = \frac{L}{qbS}$ (rolling) $\quad C_m = \frac{M}{qcS}$ (pitching) $\quad C_n = \frac{N}{qbS}$ (yawing)

Angle of set of control surface (relative to neutral position), δ. (Indicate surface by proper subscript.)

4. PROPELLER SYMBOLS

D Diameter

p Geometric pitch

p/D Pitch ratio

V' Inflow velocity

V_s Slipstream velocity

T Thrust, absolute coefficient $C_T = \frac{T}{\rho n^2 D^4}$

Q Torque, absolute coefficient $C_Q = \frac{Q}{\rho n^2 D^5}$

P Power, absolute coefficient $C_P = \frac{P}{\rho n^3 D^5}$

C_s Speed-power coefficient $= \sqrt[5]{\frac{\rho V^5}{P n^2}}$

η Efficiency

n Revolutions per second, rps

Φ Effective helix angle $= \tan^{-1}\left(\frac{V}{2\pi r n}\right)$

5. NUMERICAL RELATIONS

1 hp=76.04 kg-m/s=550 ft-lb/sec
1 metric horsepower=0.9863 hp
1 mph=0.4470 mps
1 mps=2.2369 mph

1 lb=0.4536 kg
1 kg=2.2046 lb
1 mi=1,609.35 m=5,280 ft
1 m=3.2808 ft